Journal of the Korean Physical Society, Vol. 53, No. 2, August 2008, pp. 962∼966

Observation of Single-Electron Transport in a $Zn_{0.8}Mg_{0.2}O$/ZnO Coaxial Heterostructure Nanorod

Dongchan JEONG, Dong-Keun KI, Myung-Ho BAE* and Hu-Jong LEE†
Department of Physics, Pohang University of Science and Technology, Pohang 790-784

Chul-Ho LEE, Jinkyoung YOO and Gyu-Chul YI
National Creative Research Initiative Center for Semiconductor Nanorods and Department of Materials Science and Engineering, Pohang University of Science and Technology, Pohang 790-784

(Received 21 August 2007)

Coaxial $Zn_{0.8}Mg_{0.2}O$/ZnO hetrostructure semiconducting nanorods with different band gaps were fabricated on oxide-layer-covered Si substrates by using catalyst-free metal-organic vapor-phase epitaxy. The electrical conduction of nanorods with Ti/Au Schottky-contact electrodes, taken at various temperatures down to 50 mK, revealed a Coulomb-blockade behavior, pointing a multiple quantum-dot structure existing in the ZnO nanorod core or in the $Zn_{0.8}Mg_{0.2}O$ cylindrical shell over a wide range of gate voltages. These characteristics, transformed into single-dot ones at high positive gate voltages. This study confirms, by electrical conduction measurements, the formation of a coaxial heterojunction structure between materials of two different band gaps and provides a possibility for utilizing the structure for three-terminal device applications.

PACS numbers: 84.40.Ik, 84.40.Fe
Keywords: Coaxial heterojunction nanorod, Quantum dot, Coulomb diamond

I. INTRODUCTION

Nanowires are quasi one-dimensional systems with widths comparable to the Fermi wavelength of electrons [1]. Thus, the system is suitable for studying one-dimensional quantum phenomena. Among various nanowire systems, many studies have been done on carbon nanotubes (CNTs) because they are relatively free from defects. Single-electron tunneling and phase-coherent Aharonov-Bohm oscillations were observed in CNTs [2–4]. Many studies have also been made for semiconductor nanowires made out of materials like Si, Ge, InP, and ZnO. In comparison with CNTs, semiconducting nanowires allow one easy control of electrical properties by changing the doping level. These semiconducting nanowires, with large band gaps and high carrier densities, have been applied to photonic devices [5, 6] and field-effect transistors [7,8].

Recently, interest has focused on coaxial semiconducting heterojunction nanorods with cylindrical junction interfaces, where the band modulation and its interplay with the Fermi level induce intriguing quantum phenomena. For instance, the Coulomb blockade is reported to take place in a quantum well formed in a coaxial hetrostructure nanowire consisting of different bandgap semiconductors like Ge and Si [9], where the Fermi level lies inside the Si bandgap but below the valence-band edge of Ge. Here, the Ge valence band serves as a quantum well, which may allow fabrication of high-performance devices out of *free-hole* carriers.

In this study, two coaxial $Zn_{0.8}Mg_{0.2}O$/ZnO heterojunction nanorods (A and B) are employed. The bandgap of $Zn_{1-x}Mg_xO$, determined by photoluminescence measurements, varies from 3.36 eV for $x = 0$ to 4.05 eV for $x = 0.49$. For the outside $Zn_{1-x}Mg_xO$ shell of our heterostructure nanorods with $x = 0.2$, the corresponding bandgap was 3.58 eV [10]. A two-dimensional quantum well may form along the cylindrical interface of the coaxial $Zn_{0.8}Mg_{0.2}O$/ZnO nanorod due to a band modulation of the two materials. Once the Fermi level is located inside the interfacial quantum well, under a certain suitable condition, a cylindrical shell of a two-dimensional electron gas can form along the nanorod axis. In this case, the electron gas layer is supposed to exhibit an Aharonov-Bohm-type electronic interference of the longitudinal conductance in an axial magnetic field. However, more often, the whole ZnO core may form a simple quantum well as the Fermi level resides above the height of the shallow quantum well at the interface,

*Current address: Department of Physics, University of Illinois at Urbana-Champaign, U.S.A.;
†E-mail: hjlee@postech.ac.kr; Fax: +82-54-279-5564

leaving a cylindrical electronic conducting nanorod in the ZnO core. In this study, instead of Aharonov-Bohm conductance oscillations, we observed the Coulomb blockade effect of conduction electrons, seemingly from the quantum dots (QD's) formed in the ZnO conducting core. In contrast to a simple ZnO nanorod structure, this coaxial heterojunction nanorod, in conjunction with Schottky-contact electrodes, provides a means of good carrier control in the ZnO core, which can be exploited for three-terminal field-effect-transistor-type device applications.

II. EXPERIMENT

Coaxial $Zn_{0.8}Mg_{0.2}O$/ZnO nanorods with radii from 20 to 40 nm were fabricated on Si substrates by using catalyst-free metal-organic chemical vapor deposition (MOCVD). For the fabrication of the coaxial nanorod heterostructure, ultrafine ZnO nanorods, with a diameter of about 20 nm, were employed as the core structure. The $Zn_{0.8}Mg_{0.2}O$ cylindrical-shell layer was then epitaxially grown. The total diameter of the nanorods was 30 nm for both samples. The details of the coaxial nanorod growth are described elsewhere [11]. The process was then followed by the placement of coaxial heterojunction nanorods on a new Si substrate [covered with a 300 nm-thick (1-μm-thick) Si-oxide layer for the nanorod A (B)] with pre-deposited markers. Confirming the position of a proper nanorod, the conventional e-beam lithography technique was used to prepare Ti/Au (50/60 nm thick) electrodes by thermal evaporation at a base pressure of low 10^{-6} Torr. The Si substrate itself was used as the back-gate, being capacitively coupled to the nanorod across the Si-oxide layer. For electrical transport measurements, Ti/Au electrodes were patterned on the nanorod devices as schematically shown in Figure 1(a). Room-temperature measurements were made under a high vacuum. Low-temperature measurements were carried out in a dilution fridge, which allowed for base temperatures down to 50 mK. The differential conductance was measured with the conventional lock-in technique operated at a frequency of 13.3 Hz with a modulation voltage of 50 μV superimposed on a dc bias voltage. In the following, data will be shown only for nanorod B.

III. RESULTS AND DISCUSSION

A good ohmic contact is known to be obtained for a Ti/Au electrode by rapid thermal annealing of the bilayer at 300 °C for 2 min [12]. However, in this study, no good ohmic contact was achieved in this way in spite of many attempts. Thus, the result in this report is the one obtained without thermal treatment of the contact electrodes. Figure 1(b) shows a scanning electron micrograph of nanorod B, where the spacing between the

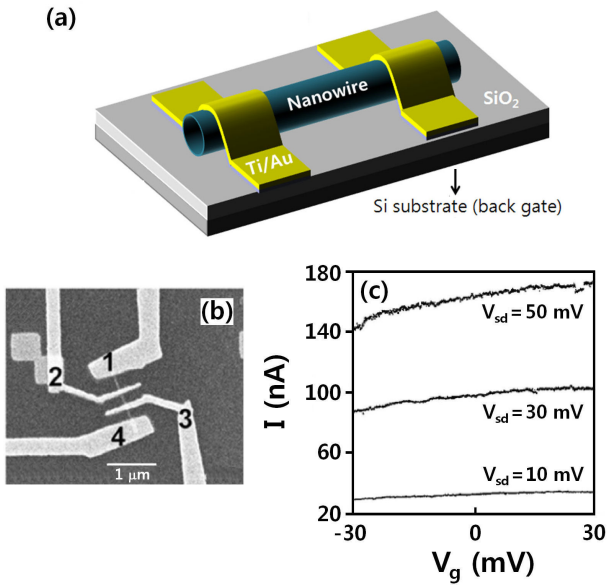

Fig. 1. (a) Schematic configuration of a coaxial $Zn_{0.8}Mg_{0.2}O$/ZnO nanorod device with two Ti/Au Schottky-contact electrodes attached. (b) An SEM image of nanorod B. Two-probe measurements were made using electrodes 2 and 3. (c) Current-voltage curves for source-drain biases of $V_{sd} = -10$, -30 and -50 mV at room temperature, which show n-type semiconducting characteristics.

two middle electrodes is 217 nm. The carrier concentration was controlled by applying a gate voltage, V_g, to the Si-substrate back-gate. Figure 1(c) shows the room-temperature current-vs-gate voltage (I-V_g) of nanorod B for three different values of the source-drain voltage, V_{sd}. This data set was taken in a *two-terminal configuration* by using the two middle gates, 2 and 3, in Figure 1(b), where the contact resistance was included. For a fixed source-drain bias voltage, the current through the nanorod increases with increasing gate voltage from -30 to 30 V, which indicates an *n-type* (or electron-carrier) semiconducting character of the ZnO core. This agrees with the picture of electrons trapped inside the cylindrical quantum well formed in the core region as the Fermi level is located above the conduction band edge of the ZnO core. The nanorod resistance, taken for $V_g = 0$, was 134 kΩ. The contact resistances of the two middle electrodes were 77 and 63 kΩ. In nanorod A, with an inter-electrode spacing of 266 nm and an oxide layer thickness of 300 nm, a similar n-type behavior was observed.

Figure 2(a) shows the current for $V_g = 0$ as a function of the bias V_{sd}, again taken in a *two-terminal configuration* by using gates 2 and 3 for temperatures ranging from 147 K to 70 mK (close to the base temperature). The I-V_{sd} curve becomes non-linear by opening a Coulomb gap for temperatures below ~40 K. Almost a full Coulomb gap opens at 70 mK. The gap is in the range of -14.5 mV $< V <$ 11 mV, which is similar to that in nanorod

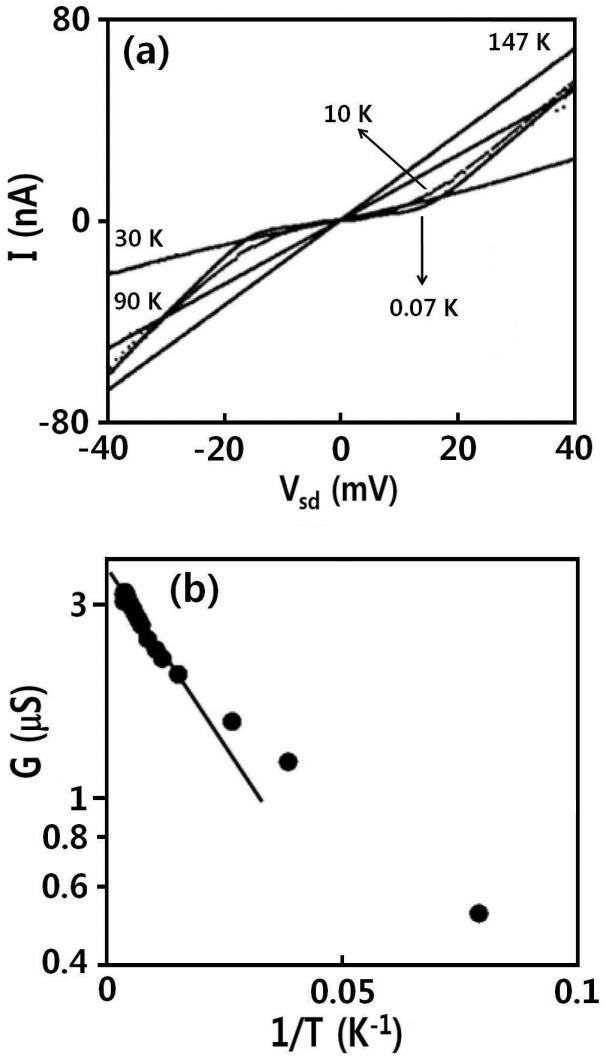

Fig. 2. (a) I-V_{sd} curves taken for $V_g = 0$ at various temperatures. Nonlinear I-V_{sd} characteristics begin to occur for temperatures below ∼30 K. (b) The zero-bias conductance, taken at a the bias current of 1 nA through electrodes 1 and 4, as a function of inverse temperature. The solid line represents the best fit of the conductance to the thermally activated injection of conducting carriers to the ZnO core over the Schottky potential barrier E_a; $G(T) \sim \exp(-E_a/k_BT)$.

A, *i.e.*, -14 mV $< V <$ 12 mV.

The high contact resistance and the increase in its value with decreasing temperature point to the formation of a Schottky barrier between the metallic Ti layer and the cylindrical shell of semiconducting $Zn_{0.8}Mg_{0.2}O$. Electron carriers are injected into the ZnO core over the Schottky barrier by the thermal activation at finite temperature. Figure 2(b) shows the zero-bias conductance as a function of the inverse temperature. This data set was taken in a *four-terminal configuration*, excluding the contact resistance. The zero-bias conductance, decreasing from 3.29 μS at 287 K to 95 nS at 4.3 K, exhibits a good fit to the thermal-activation dependence of $G(T) \sim \exp(-E_a/k_BT)$ at high temperatures, but tends to deviate from this temperature dependence for temperatures below ∼40 K. Here, E_a is the thermal activation energy corresponding to the Schottky barrier height [13]. The best-fit value of E_a is 3.4 meV, which corresponds to a thermal activation temperature of $T_a = E_a/k_B \simeq$ 40 K. This Schottky barrier height is about 1000 times smaller than the gap size of ZnO. Thus, the electron carrier density of the ZnO core is determined by thermally activated carrier injection from the $Zn_{0.8}Mg_{0.2}O$ layer or the electrodes rather than from its valence band. In other words, thermal injection of carriers from outside of the ZnO core dominates the electron transport of the ZnO core rod itself at temperatures above 40 K. At temperatures below 40 K, carrier injection by the quantum tunneling of electron through the Schottky barrier may become the major carrier- or conduction-control mechanism, which explains the deviation of the conductance from the thermal-activation behavior in Figure 2(b) in the low-temperature region.

The differential conductance was observed to oscillate periodically as functions of V_g and V_{sd}, which resembles the Coulomb-blockade behavior in a quantum-dot structure. Electron-confinement states may have formed in a narrow region, which acted as a quantum dot (QD), between two middle gates. The electron-confinement state can be sensitively revealed in the electrical conductance by even a slight imperfection in the nanorod or by the presence of Mg dopant atoms in the $Zn_{0.8}Mg_{0.2}O$ shell. Periodic resonant conductance enhancement occurred when the gate voltage was varied as the Fermi level matched the quantized levels separated by the charging energy. An ideal Coulomb diamond structure would be obtained from a single QD [9]. As shown in Figure 3(a), however, our nanorod system did not show an ideal diamond structure; the conductance did not oscillate at zero V_{sd} for most gate voltages examined. In addition, the Coulomb diamond structure appeared in multiples and was irregular, suggesting formation of multiple QD's along the nanorod [14,15]. This feature was reproducible for repeated measurements in both nanorod samples.

The largest Coulomb diamond in Figure 3(a) is thought to be caused by multiple QD's. The wide ΔV_{sd} with a large zero-conductance area implies that more than one QD is connected in series. The gate capacitance C_g can be calculated from $C_g = e/\Delta V_g$, where ΔV_g is the width of the gate voltage of a single Coulomb diamond; $C_g = 0.064$ aF (for nanorod B).

A high-enough positive gate voltage may transform the multiple QD behavior into a single QD one as the Fermi level is enhanced above the potential irregularities. The resulting quantum states are supposedly well extended along the nanorod. This transformation has already been observed in semiconducting nanorods and carbon nanotubes [14,15]. Effective merging of multiple dots into a single QD is evidenced in our nanorod B for high gate voltages from 17 to 26 V in Figure 3(a), as can be signified by the formation of the degeneracy points

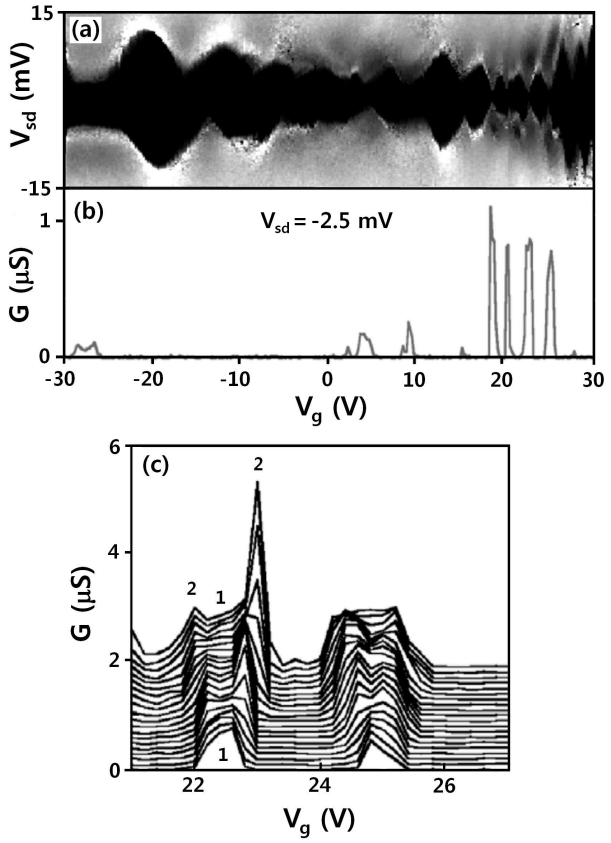

Fig. 3. (a) Gray-scale plot of the differential conductance as a function of V_g and V_{sd} at 50 mK. The black and the bright areas are the zero-conductance and the finite-conductance regions, respectively. (b) A part of the gray-scale plot for $V_{sd} = -2.5$ mV. (c) Conductance *vs* V_g graph, for different V_{sd} ranging from -2.0 mV to -3.9 mV in steps of -0.1 mV from bottom to top.

with very clear periodic conductance peaks at $V_{sd} = -2.5$ mV [Figure 3(b)]. The charging energy $E_c = e\Delta V_{sd}$ estimated from the height of the diamond in this gate voltage range turns out to be 4 meV. The total capacitance C of the presumed QD structure estimated from the slope of the diamond, following the relation [16]

$$\Delta V_g = \frac{C}{eC_g}\left(\Delta E + \frac{e^2}{C}\right), \qquad (1)$$

is 35.5 aF. Here, ΔE is the level spacing discussed below. The high ratio of C/C_g, 550, corresponding to the geometrical factor of gating the nanorod, indicates that back-gating should be extremely difficult.

In Figure 3(c), the variation of two conductance peaks was examined in detail for the gate voltages ranging from 21 to 27 V. The lowest trace was taken at $V_{sd} = -2.0$ mV. The two conductance peaks are a part of the normal Coulomb peaks. Thus, aside from the geometrical factor, the gate voltage between the two peaks should correspond to the energy required to add an electron to a QD. More than one quantized energy states can contribute to the source-drain conductance for a high bias V_{sd}, as V_{sd} becomes larger than the spacing between the quantized levels, ΔE. This leads to a splitting of the Coulomb peak into multiple minor peaks as the ones denoted by the number 2 in Figure 3(c). The observed excitation energy, $\Delta E = 0.5$ meV, in Figure 3(c) is a few tens of times smaller than the charging energy [16], which is consistent with the usual energetics of the space-confinement-induced quantized level difference and the charging energy in a QD.

IV. CONCLUSION

Electrical transport measurements on coaxial heterostructure $Zn_{0.8}Mg_{0.2}O$/ZnO nanorods with Ti/Au Schottky-contact electrodes reveal the formation of a quantum well in the ZnO cylindrical core. Electron carriers were injected through the Schottky barrier formed between the metallic electrodes and the outer $Zn_{0.8}Mg_{0.2}O$ shell into the ZnO nanorod core, by thermal activation at high temperatures ($T \gtrsim 40$ K) and presumably by quantum tunneling at low temperatures ($T \lesssim 40$ K). No observation of Aharonov-Bohm conductance interference in our samples A and B rules out the formation of a cylindrical two-dimensional electronic gas layer at the interfacial shallow potential well. Instead, conductance oscillations were observed at low temperatures due to the Coulomb blockade of electron conduction at a serially connected multiple QD structure, which was presumably formed in the ZnO nanorod core or in $Zn_{0.8}Mg_{0.2}O$ cylindrical shell between the two Schottky-contact electrodes with high contact resistances of 77 and 63 kΩ. A charging energy of 4 meV was obtained from the clearly defined Coulomb diamond.

If it had not been for the outer $Zn_{0.8}Mg_{0.2}O$ cylindrical shell, electron carriers could not have been easily added to the ZnO core because of the high conduction band edge and the wide Schottky barrier. Thus, the $Zn_{0.8}Mg_{0.2}O$ layer was essential for efficient injection of the electron carriers and turned the ZnO core into an n-type semiconducting rod. A local gate on top of this coaxial nanorod would provide a convenient means to control the carrier density at the nanorod for three-terminal-device applications, especially for a high bias range where the multiple-QD effect can be eliminated.

ACKNOWLEDGMENTS

This work (for HJL) was supported by the Electron Spin Science Center in Pohang University of Science and Technology, by a Pure Basic Research grant R01-2006-000-11248-0 administered by Korea Science and Engineering Foundation, by a Korea Research Foundation grant (KRF-2005-070-C00055), and by the POSTECH

Core Research Program. GCY was supported by the National Creative Research Initiative Project (R16-2004-004-01001-0) of KOSEF. MHB was supported by the Korea Research Foundation Grant No. KRF-2006-352-C00020.

REFERENCES

[1] T. Heizel, *Mesoscopic Electronics in Solid State Nanostructure* (WILEY-VCH, Weinheim, 2003), p. 165.
[2] J.-R. Kim, J.-J. Kim and J. Kim, J. Korean Phys. Soc. **51**, 2094 (2007).
[3] M. Bockrath, D. H. Cobden, P. L. McEuen, N. G. Chopra, A. Zettl, A. Thess and R. E. Smalley, Science **275**, 1922 (1997).
[4] A. Bachtold, C. Strunk, J. P. Salvetat, J. M. Bonard, L. Forró, T. Nussbaumer and C. Schönenberger, Nature **397**, 673 (1999).
[5] W. I. Park and G.-C. Yi, Adv. Mater. **16**, 89 (2004).
[6] S.-H. Jeong, K.-H. Park and H.-J. Song, J. Korean Phys. Soc. **50**, 1692 (2007).
[7] J. Xiang, W. Lu, Y. Hu, Y. Wu, H. Yan and C. M. Lieber, Nature **441**, 489 (2006).
[8] H. Oh, Y.-S. Lo, J.-J. Kim, J.-O. Lee and S. S. Kim, J. Korean Phys. Soc. **51**, 2094 (2007).
[9] W. Lu, J. Xiang, B. P. Timko, Y. Wu and C. M. Lieber, Proc. Natl. Acad. Sci. U.S.A. **102**, 10046 (2005).
[10] W. I. Park, G.-C. Yi and H. M. Jang, Appl. Phys. Lett **79**, 2022 (2001).
[11] W. I. Park, J. Yoo and D. W. Kim, J. Phys. Chem. B **110**, 1516 (2006).
[12] S. Y. Kim, H. W. Jang, J. K. Kim, C. M. Jeon, W. I. Park, G.-C. Yi and J.-L. Lee, J. Electron. Mater **31**, 868 (2002).
[13] B.-K. Kim, J.-O. Lee and J.-J. Kim, J. Korean Phys. Soc. **46**, 1262 (2005).
[14] C. Thelander, T. Mårtensson, M. T. Björk, B. J. Ohlsson, M. W. Larsson, L. R. Wallenberg and L. Samuelson, Appl. Phys. Lett. **83**, 2052 (2003).
[15] J.-R. Kim, B.-K. Kim, S.-R. Kim, J.-J. Kim, J.-O. Lee and J. H. Kim, J. Korean Phys. Soc. **49**, 1694 (2006).
[16] L. L. Sohn, L. P. Kouwenhoven and G. Schön, *Mesoscopic Electron Transport* (Kluwer Academic Publisher, Dordrecht, 1997), p. 105.